Comparison of metal erosion characteristics due to arc in Air and SF_6

M. SATO[1], K. HORINOUCHI[1], and D. YOSHIDA[2]

[1] *Advanced Technology R&D Center, Mitsubishi Electric Corporation*
Amagasaki, 661-8661, Japan
[2] *Transmission & Distribution System Center, Mitsubishi Electric Corporation*
Amagasaki, 661-8661, Japan
e-mail address: Sato.Motohiro@dr.mitsubishielectric.co.jp

ABSTRACT

Erosion of metal enclosure due to electric arc was investigated to clarify the effect of the usage of different gas for internal arc tests in high-voltage switchgear. Since SF_6 gas, which is commonly used in the high-voltage switchgear, has a potential to give negative impact on the environment, alternative testing using Air has been in discussion worldwide. Erosion characteristics of the metal enclosure due to the internal arc is crucial to establish test method with Air which gives equivalent test results to the testing with SF_6.

Experimental investigation of the internal arc is conducted with different insulating gases (SF_6 and Air) and different enclosure materials. Comparison of visual inspection, geometrical analysis, elementary analysis and cross-sectional observation indicate that erosion of enclosure is caused by the following two steps and predominant factor.

(i) Melting of metal enclosure
- In Air, energy injected by the heat transfer from the arc affects the amount of the molten metal.
- In SF_6, chemical reaction energy on the metal affects the amount of the molten metal.

(ii) Spattering of molten metal
Impact pressure of the arc jet affects the spattering degree on the enclosure. The pressure depends on the arc diameter.

1. INTRODUCTION

Internal arc faults can occur inside metal-enclosed high-voltage switchgear. When an internal arc is ignited in the switchgear, it travels in the enclosure due to the magnetic force caused by the fault current, raises the gas pressure, and makes a hole on the enclosure wall. This phenomenon is called burn-through.

SF_6 gas insulated switchgears, which are commonly used in high-voltage power systems, are designed so that the burn-through doesn't occur due to internal arc, and their performance needs to be verified by internal arc tests.

On the other hand, internal arc tests with SF_6 gas negatively impact on the environment, because SF_6 is vented into the atmosphere when the burn-through occurs. Global warming potential (GWP) of SF_6 is 23,900 times larger than that of CO_2. Since GWP of the Air is zero, alternative internal arc tests using Air have been in discussion. Erosion characteristics of the metal enclosure due to the internal arc is crucial, and have been investigated in Air and SF_6 with various conditions [1][2]. However, no comparison of their characteristics is reported on the same condition.

This paper reports experimental investigation results of metal erosion characteristics due to the arcs in Air and SF_6 assuming various enclosure materials.

2. EXPERIMENTAL SET-UP

Rod-plate electrode configuration was applied to simulate the internal arc in the metal enclosure. Fig. 1 shows experimental apparatus for investigation. Parallel conductors were placed to supply the test current so that the current path is alighted to the arc current to avoid the effect of the magnetic force to achieve stable arc. The enclosure was filled with Air or SF_6 (0.6 MPa-abs).

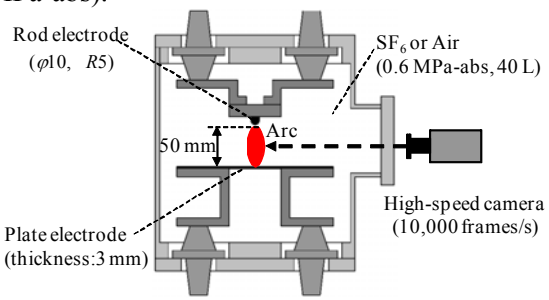

Fig. 1 Experimental apparatus

Three materials such as copper-tungsten (CuW), steel (Fe), and aluminium (Al) were used for the electrodes. Test condition on the combination of electrode material is shown in Table 1. These

electrodes were connected with a copper fuse of 0.5 mm diameter.

Resonant LC circuit was used to supply alternating current to the apparatus. Fig. 2 shows an example of the waveform of the test current and test voltage. Test frequency was 60 Hz, and test current was 10 kArms at the first half cycle. Since measured test voltage was constant regardless of test current, the arc seems to be stable without motion between the electrodes.

High-speed camera (10,000 frames/s) was placed outside the enclosure to record the physical behaviour of the arc through the window. Visual observation results also show that motion of the arc is very small and the arc can be considered to be stable.

Table 1 Combinations of electrode material

	Rod electrode (simulated conductor)	Plate electrode (simulated enclosure)
Case 1	CuW	Fe
Case 2	Al	Fe
Case 3	Al	Al

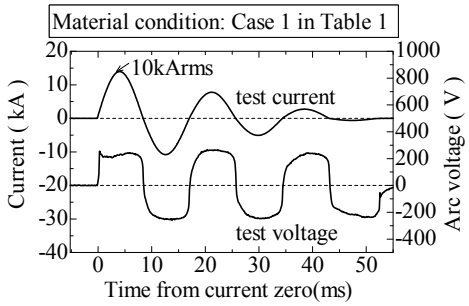

Fig. 2 Test waveforms with Air

3. OBSERVATIONS OF ELECTRODES AFTER EXPERIMENTS

3.1 Visual inspection

Erosion of the rod and plate electrodes was visually inspected after the experiments. Table 2 shows pictures of those electrodes. The deepest point of the erosion was around the center of the plate electrodes in all conditions. The molten metal spattered from the eroded area to the outside, and the diameter of spattering in Cases 2 and 3 was smaller than that in Case 1.

Different erosion was observed on the rod electrodes. While CuW electrodes almost maintained their initial shape, erosion of Al electrodes were approximately 3mm.

3.2 Erosion depths of plate electrodes

Erosion depths of the plate electrodes were measured to evaluate the degree of erosion in each case quantitatively. Measured results are shown in Fig. 3. In Case 1, erosion depth in Air was approximately 2 mm which is approximately twice larger than that in SF_6. On the other hand, erosion depth in Air was less than that in SF_6 in Case 2 and Case 3 where Al rod electrode was applied. While the erosion of Fe plate electrode was small in Case 2, it becomes much larger when Al plate electrode was applied in Case 3, and a penetration on plate electrode with 3 mm thick occurred when the test was performed in SF_6.

Table 2 Erosion of electrodes after experiment

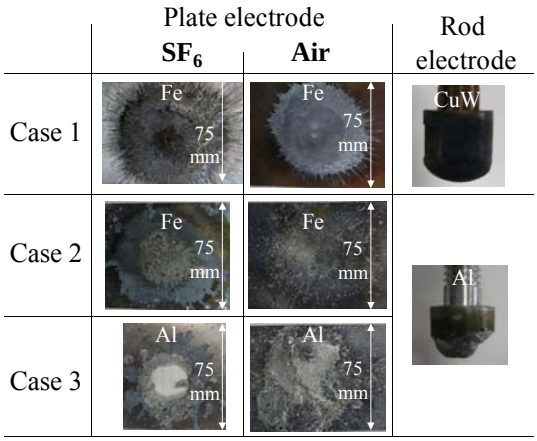

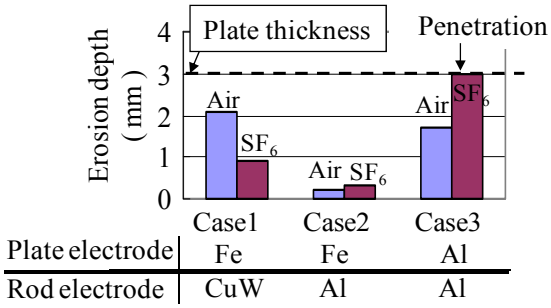

Fig. 3 Erosion depths of plate electrodes

3.3 Elementary analysis at eroded area

Chemical elements at the eroded area on the plate electrodes were investigated quantitatively using SEM/EDX analysis to study the presence of the chemical reactions between metal and gas. The analysis results of the detected elements in each case are shown in Table 3. They are shown as relative values compared to the plate electrode material.

(i) Materials of the rod electrodes were detected in Case 1 and 2. The detected ratio of the rod electrode material in Case 2 (Al) was more than 6 times larger than that in Case 1 (Cu or W).

(ii) Chemical elements related to gases were detected in all cases. A large amount of F was detected when the test was done in SF_6.

Table 3 Chemical elements at eroded area on plate electrodes

Materials of electrodes	Gas species	Atomic composition on plate electrodes surface
Case 1 Rod: CuW Plate: Fe	SF_6	Fe : Cu : W : S : F =1 : 0.01 : 0 : 0 : 0.99
	Air	Fe : Cu : W : N : O =1 : 0.01 : 0.12 : 0 : 0.63
Case 2 Rod: Al Plate: Fe	SF_6	Fe : Al : S : F = 1 : 0.79 : 0 : 4.5
	Air	Fe : Al : N : O =1 : 1.1 : 0 : 1.45
Case 3 Rod: Al Plate: Al	SF_6	Al : S : F =1 : 0.01 : 3
	Air	Al : N : O =1 : 0.05 : 0.49

3.4 Cross-sectional observations

Eroded areas of the plate electrodes were cut to observe the cross-sectional areas to clarify the depth of the melted material. Surface layers of the eroded areas showed different elemental composition, and the measured thickness of the layers distributed from 1 to 20 μm.

4. DISCUSSION

Different phenomena of the erosion of metal plate electrode were considered to specify the predominant factor of the erosion in different electrode material and different gas. The experimental results show that following phenomena are related to the erosion characteristics:

(a) Melting of metal by the heat due to the energy of the arc
(b) Melting of metal by chemical reaction around the eroded area
(c) Spattering of the molten metal

Fig. 4 shows the estimated process of the metal erosion due to the arc for each phenomenon.

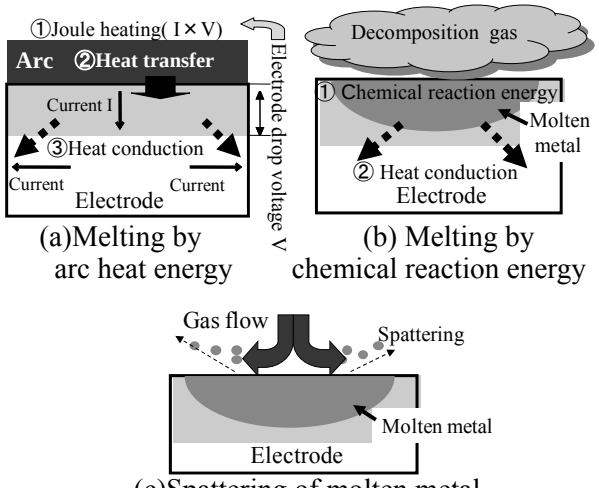

(a)Melting by arc heat energy

(b) Melting by chemical reaction energy

(c)Spattering of molten metal

Fig. 4 Mechanism of arc erosion of metal

4.1 Melting of metal by the heat due to the arc energy

Electrode drop voltage mainly affects the arc energy and the melting of the surface of the electrode. Fig. 4 (a) shows the process of the melting of the electrode by the heat of the arc. Joule energy generated by the arc current and the electrode drop voltage transfers to the surface of the electrode and melts metallic material. Since electrode drop voltage is almost the same among the type of the gas [3], the melting of the metal due to the arc energy mainly depends on the heat transfer from the arc to the electrode.

Heat transfer depends on gas properties around the arc. The vertical gas flow from the rod electrode to the plate electrode is observed by the high-speed camera during the experiments. It is considered to be an impinging arc jet streaming from the rod electrode to the plate electrode. In the impinging jet condition, heat transfer coefficient h is shown as the following equation [4]:

$$Nu_b = 0.535\, Pr^{0.4} Re^{0.5} \quad (N_{ub} = hb_0 / k) \tag{4.1}$$

$$bo = R_a \tag{4.2}$$

$$u = u_{arc} = \sqrt{\mu_0 I \times J /(2\pi\rho_{arc})} = I /(\pi R_a)\sqrt{\mu_0 /(2\rho_{arc})} \tag{4.3}$$

$$h = 0.535\, \underbrace{k\left(\frac{\eta Cp}{k}\right)^{0.4}\left(\frac{\rho_{arc}}{\eta^2}\right)^{0.25}}_{\mathrm{A}}\left(\frac{I\sqrt{\mu_0/2}}{\pi b_0 R_a}\right)^{0.5} \tag{4.4}$$

where Nu_b is Nusselt number, Pr is Prandtl number, Re is Reynolds number, k is the thermal conductivity, and b_o is the diameter of the rod electrode, R_a is the arc diameter, u is the gas flow velocity, u_{arc} is the arc jet velocity, μ_0 is the magnetic permeability in a vacuum, I is the current value, J is the current density, ρ_{arc} is the arc density, η is the coefficient of the viscosity and Cp is specific heat at a constant pressure.

Heat transfer coefficient h depends on the part "A" of Eq. (4.4) in the same geometric condition, and "A" is determined by the gas properties. At a temperature range higher than 5,000 K, "A" of Air exceeds that of SF_6, since η of Air is less than a one-hundredth of that of SF_6. At 15,000 K, which is assumed as the temperature at the center of the arc, "A" is 2.6 times larger for Air than for SF_6. As a result, the heat transfer from the arc to the plate electrode is higher in Air than in SF_6. This result is in good agreement with the experimental results in Case 1.

4.2 Melting of metal due to chemical reaction energy at eroded area

Chemical reaction energy becomes very large when the arc is generated on Al electrodes in SF_6. Fig. 4 (b) shows the process of the melting of the electrode by chemical reaction energy of gas and molten metal. The reaction energy was investigated considering the compounds as a result of the chemical reaction and their standard enthalpy of formation for each gas and electrode condition [5]. The following assumption was also considered for investigation:

(a) Metal at the eroded area is molten (liquefied).
(b) Gas near the eroded area is atomized by arc heat.
(c) All of the detected elements at the arc eroded area bond with each other.
(d) Fe_2O_3 and Fe_3O_4 are produced with the ratio of 1:2[6].
(e) F_2Fe and F_3Fe are produced with the ratio of 3:2.
(f) Reaction with W and O are ignored, because very little amount of them are detected at the experiment.
(g) Gases preferentially react with Al compared to Fe.

Table 4 shows chemical reaction considered in the investigation and calculated energy. The calculated energy is larger in SF_6 than that in Air especially in Cases 2 and 3, because the reaction energy of F and Al is extremely higher than the other reaction. It is approximately 4.5 times larger in SF_6 than in Air especially in Case 3, resulting in the penetration of Al plate electrode when the arc is generated in SF_6.

Table 4 Chemical reaction and energy

		Estimated chemical reaction equations from Table 2	Energy (kJ/mol)
Case 1	SF_6	$Fe + F \Rightarrow 0.58\,Fe + 0.25\,F_2Fe + 0.17\,F_3Fe$	438
	Air	$Fe + 0.63\,O \Rightarrow 0.55\,Fe + 0.06\,Fe_2O_3 + 0.11\,Fe_3O_4$	335
Case 2	SF_6	$Fe + 0.79\,Al + 4.5\,F \Rightarrow 0.11\,Fe + 0.53\,F_2Fe + 0.36\,F_3Fe + 0.79\,AlF_3$ (Estimated from Case3)	2319
	Air	$Fe + 1.1\,Al + 1.45\,O \Rightarrow 0.33\,Fe + 0.74\,Al + 0.08\,Fe_2O_3 + 0.17\,Fe_3O_4 + 0.18\,Al_2O_3$ (Estimated from Case 3)	932
Case 3	SF_6	$Al + 3\,F \Rightarrow AlF_3$	1760
	Air	$Al + 0.49\,O \Rightarrow 0.68\,Al + 0.16\,Al_2O_3$	394

4.3 Spattering of the molten metal

Impact pressure of the arc jet also seems to be related to the spattering. Fig. 4 (c) shows that the impinging jet streaming from the rod electrode to the plate electrode caused the spattering of molten metal. Impact pressure P_i is calculated with the following formula:

$$P_i = \frac{1}{2}\rho_{arc} u_{arc}^{\ 2} = \frac{\mu_0}{4}\left(\frac{I}{\pi R_a}\right)^2 \qquad (4.5)$$

P_i becomes smaller when Al is used for the rod electrode, because R_a of the arc jet was reported to be larger than that with the electrodes made of other material [7]. This phenomenon results in the small diameter of spattering that is observed in Case 2 and Case 3. This also results in a small erosion depth in Case 2 which is less than a one-third of in Case 1.

5. CONCLUSION

The difference of metal erosion characteristics due to the arc was studied for different type of gas and different electrode material. The following results were given by the experiments with the rod-plate electrodes configuration:

(i) Energy injected into electrodes by heat transfer from the arc in Air is more than twice of that in SF_6, and is the predominant factor that affects the melting of metal.
(ii) Chemical reaction energy becomes predominant when the electrode material is Al and the gas is SF_6. It is more than 4 times as large as that in Air.
(iii) Gas flow from a rod electrode with impact pressure spatters the molten metal on the plate electrode. The diameter of the spattering area depends on the material of the rod electrode.

REFERENCES

[1] H. Kuwahara, "Fundamental Investigation on Internal Arcs in SF_6 Gas-Filled Enclosure", IEEE Trans, Vol.PAS-101, No. 10, 1984

[2] H. Fukagawa, "High Current Arc Phenomena and its Countermeasures on Transmission and Distribution Lines", CRIEPI Research Report, W04, 1989 (in Japanese)

[3] Y. Yokomizu, "Electrode sheath voltages for helium arcs between non-thermionic electrodes of iron, copper and titanium", J. Phys. D: Appl. Phys. 31, pp 880-883, 1998

[4] Gardon, R. and Akfirat, J. C., "Heat Transfer Characteristics of impinging Two-dimensional Jets", Trans.ASME, J. Heat transfer, pp 101-108, 1966

[5] NIST, "Search for Species Data by Chemical Formula", http://webbook.nist.gov/chemistry/form-ser.html

[6] T. Miyagi, "Influence of Arc Current on Energy Balance due to High Current Arc in a Closed Chamber", IEEJ Transactions on Power and Energy, Volume 130, Issue 2, pp 232-238, 2010 (in Japanese)

[7] S. Tanaka, "Flow Velocity Characteristics of High Current Arc Jet in Atmospheric Air (Part2)", CRIEPI Research Report, W01021, 2002 (in Japanese)